**Supplementary material**

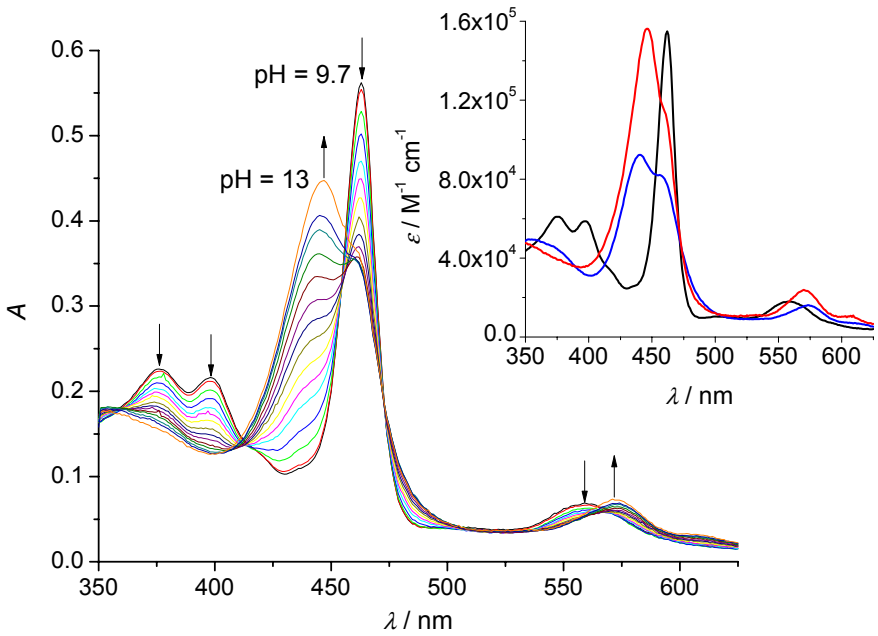


**Figure S1**. A typical titration profile of 3.6 μM $Mn^{III}$TE-3-PyP in 2 M $NaClO_4$ with 0.2 M NaOH ($\theta$ = 25 °C, $l$ = 1 cm). The pH values of the solution were varied within the pH-range 9.7-13 (for the sake of clarity not all measured spectra are shown). **Inset:** The theoretical spectra of the protonated, (——), mono-deprotonated (——), and double deprotonated (——) species.

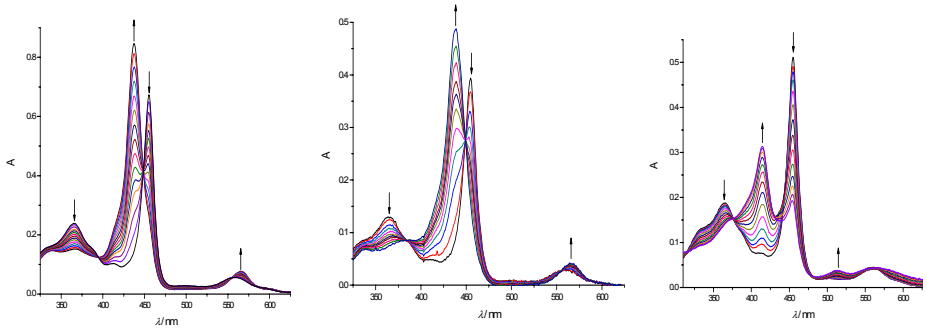

**Figure S2.** Time-dependent spectral changes of $Mn^{III}$TE-2-PyP in an anaerobic cell. **Left:** Condition: [$Mn^{III}$TE-2-PyP] = 49 μM, **pH = 8** (0.05 M $NaH_2PO_4$), $I$ = 0.1 M (NaCl), $\theta$ = 25 °C, $l$ = 0.1 cm, $E_{cell}$ = -450 mV *vs.* Ag/AgCl. **Middle:** Condition: [$Mn^{III}$TE-2-PyP] = 29 μM, **pH = 4** (0.05M $CH_3COONa$), $I$ = 0.1 M (NaCl), $\theta$ = 25 °C, $l$ = 0.1 cm, $E_{cell}$ = -450 mV *vs.* Ag/AgCl. **Right:** Condition: [$Mn^{III}$TE-2-PyP] = 37 μM, **pH = 1.5**, $I$ = 0.1 M (NaCl), $\theta$ = 25 °C, $l$ = 0.1 cm, $E_{cell}$ = -450 mV *vs.* Ag/AgCl

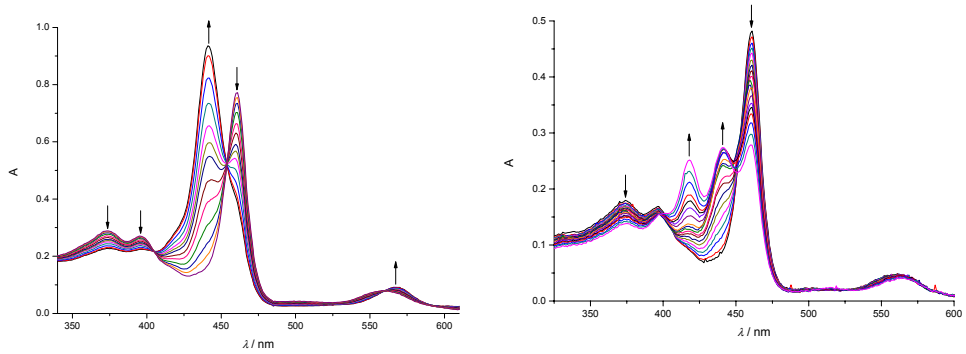


**Figure S3.** Time dependent spectral changes of $Mn^{III}$TE-3-PyP in an anaerobic cell. **Left:** Condition: [$Mn^{III}$TE-3-PyP] = 50 μM, **pH = 9** (0.025M $Na_2B_4O_7$), $I$ = 0.1 M (NaCl), $\theta$ = 25 °C, $l$ = 0.1 cm, $E_{cell}$ = -600 mV *vs.* Ag/AgCl. **Right:** Condition: [$Mn^{III}$TE-3-PyP] = 31 μM, **pH = 4** (0.05M $CH_3COONa$), $I$ = 0.1 M (NaCl), $\theta$ = 25 °C, $l$ = 0.1 cm, $E_{cell}$ = -600 mV *vs.* Ag/AgCl.

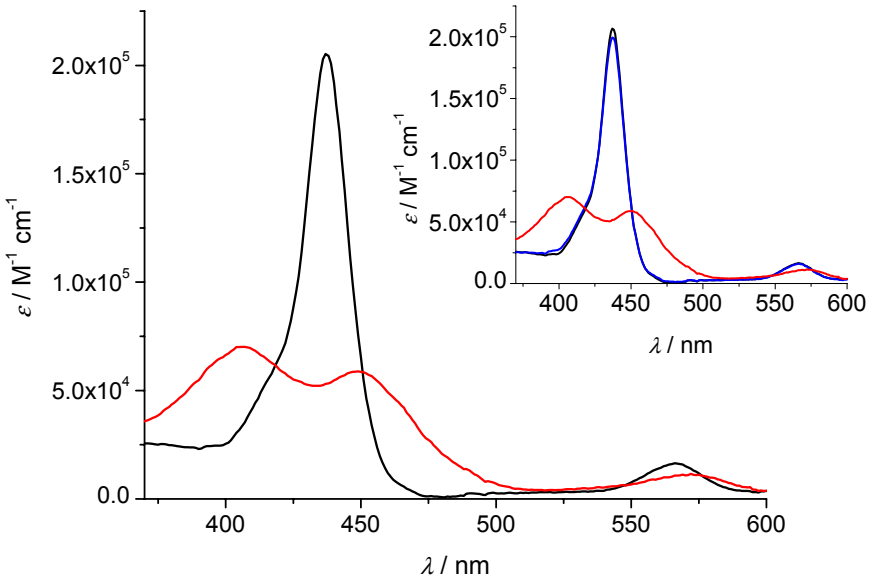


**Figure S4.** The theoretical spectra of the protonated (——) and deprotonated (——) species of $Mn^{III}$TE-2-PyP predicted according to the 2-species model. **Inset**: The theoretical spectra of the fully protonated (——), monodeprotonated (——), and fully deprotonated (——) species predicted according to the 3-species model.

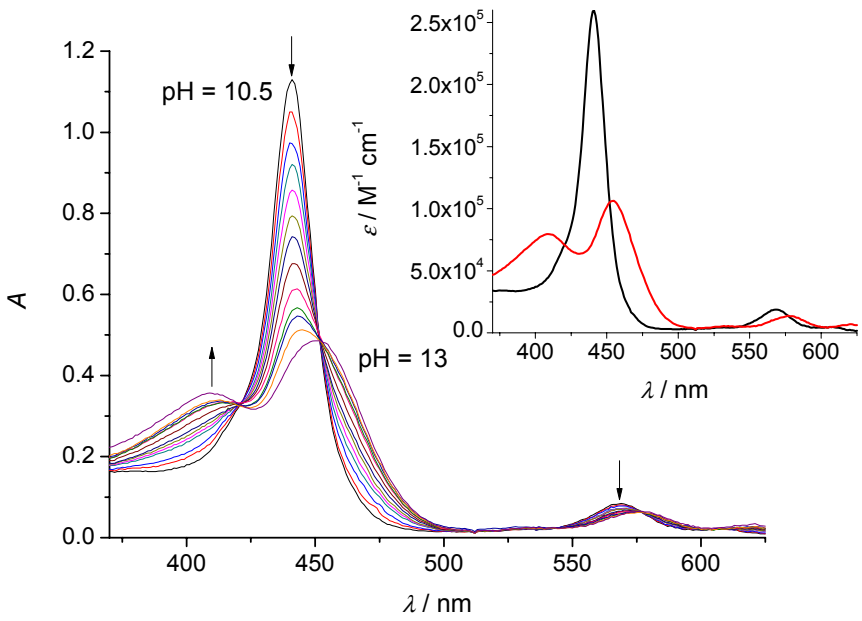


**Figure S5.** A typical titration profile of 4 μM $Mn^{II}$TE-3-PyP in 2 M $NaClO_4$ with 0.2 M NaOH ($\theta$ = 25 °C, $l$ = 1 cm). The pH values of solution were varied within the pH-range 10.5-13.0 (for the sake of clarity not all measured spectra are shown). **Inset:** The theoretical spectra of the protonated (——) and deprotonated (——) species predicted according to the 2-species model. Spectra obtained at pH < 10.5 are shown in Figure S8.

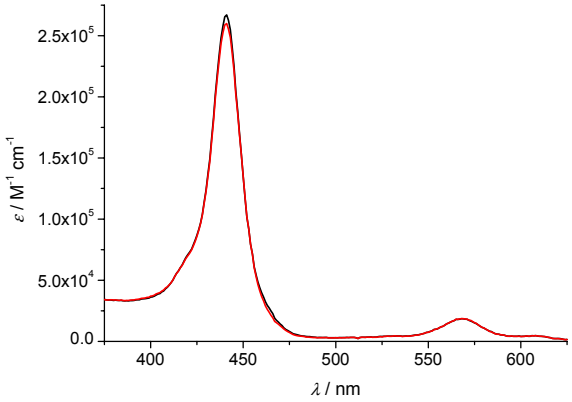


**Figure S6.** The theoretical spectra of $Mn^{II}$TE-3-PyP species obtained from the spectral changes observed in the spectroelectrochemical experiment at pH 9 (——) and in the pH-titration of $Mn^{III}$TE-3-$PyP^{5+}$ in the presence of ascorbic acid recorded at pH 10.5. (——).

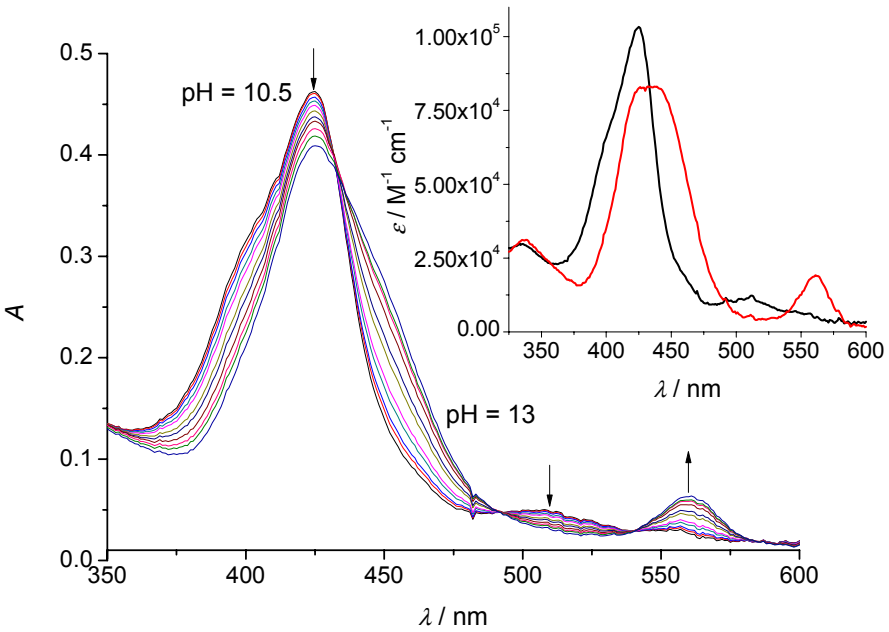


**Figure S7.** A typical titration profile of 4.8 μM $Mn^{IV}$TE-3-PyP in 2 M $NaClO_4$with 0.2 M NaOH ($\theta$ = 25 °C, $l$ = 1 cm) in the presence of 0.1 mM $[Mo(CN)_8]^{3-}$. The pH values of the solution were varied within the pH-range 10.5-13. (for the sake of clarity not all measured spectra are shown). **Inset:** The theoretical spectra of the protonated (——) and deprotonated (——) species.

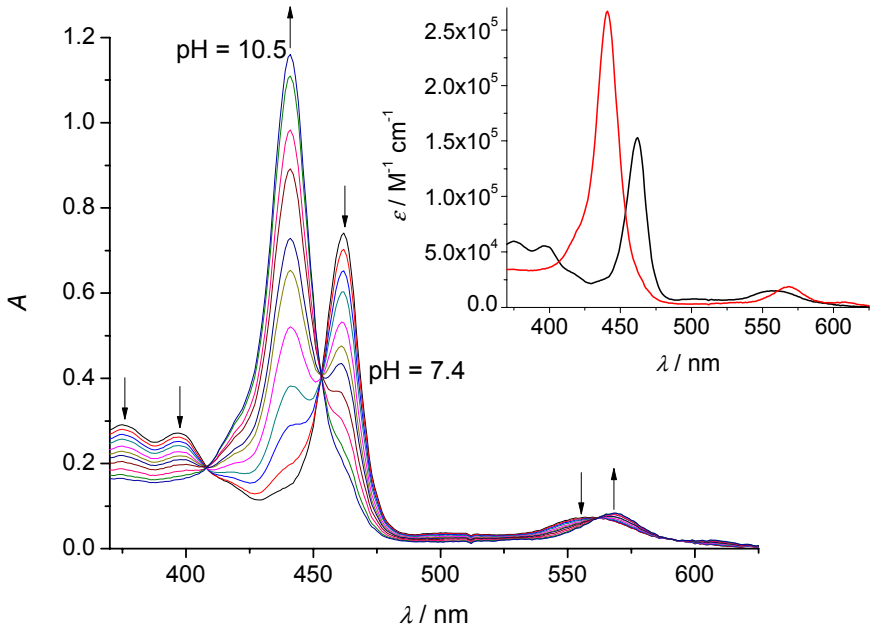


**Figure S8.** A typical titration profile of (4 μM $Mn^{III}$TE-3-PyP + 20 mM ascorbic acid + 0.5 mM $[Fe(CN)_6]^{3-}$) in 2 M $NaClO_4$with 0.2 M NaOH ($\theta$ = 25 °C, $l$ = 1 cm). The pH values were varied within the pH-range 7.4-10.5 (for the sake of clarity not all measured spectra are shown). **Inset:** The theoretical spectra of $(H_2O)_2Mn^{III}$TE-3-$PyP^{5+}$ (——) and $(H_2O)_2Mn^{II}$TE-3-$PyP^{4+}$ (——).

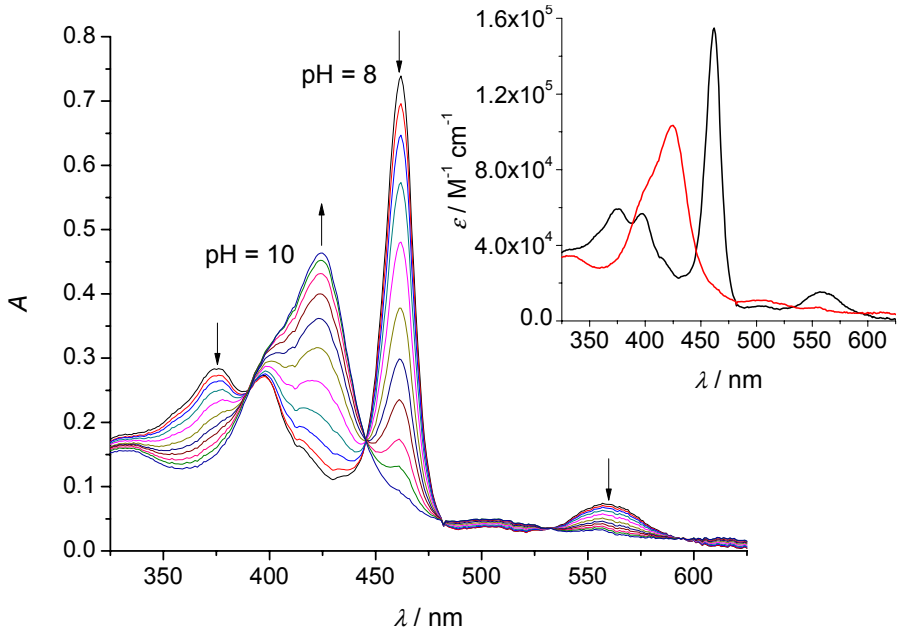


**Figure S9.** A typical titration profile of 4.8 μM $Mn^{III}$TE-3-PyP in 2 M $NaClO_4$ with 0.2 M NaOH ($\theta$ = 25 °C, $l$ = 1 cm) in the presence of 0.1 mM $[Mo(CN)_8]^{3-}$ and 0.1 mM $[Mo(CN)_8]^{4-}$. The pH values of the solution were varied within the pH-range 8-10 (for the sake of clarity not all measured spectra are shown). **Inset:** The theoretical spectra of the reduced (——) and oxidized forms of MnTE-3-PyP (——).

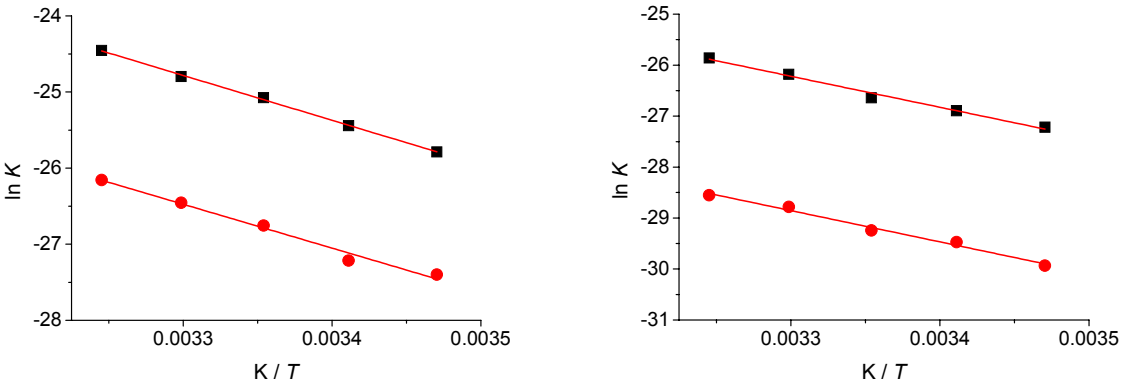


**Figure S10.** van't Hoff plots for deprotonation constants of $Mn^{III}$Ps, $K_{a1}$ (■) and $K_{a2}$ (●), $I$ = 2 M ($NaClO_4$): **left:** $Mn^{III}$TE-2-PyP, **right:** $Mn^{III}$TE-3-PyP.

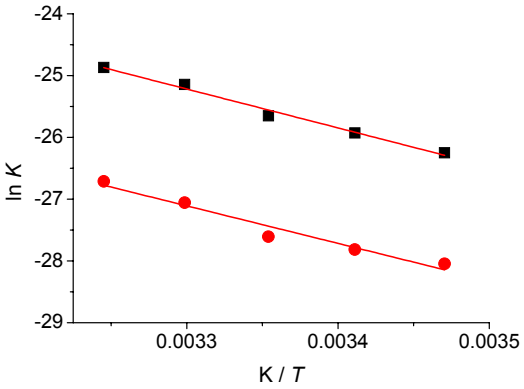


**Figure S11.** van't Hoff plots for deprotonation constants $K''_{a1}$ of $Mn^{IV}$Ps, $I$ = 2 M ($NaClO_4$): $Mn^{IV}$TE-2-Pyp (■),$Mn^{IV}$TE-3-Pyp (●).

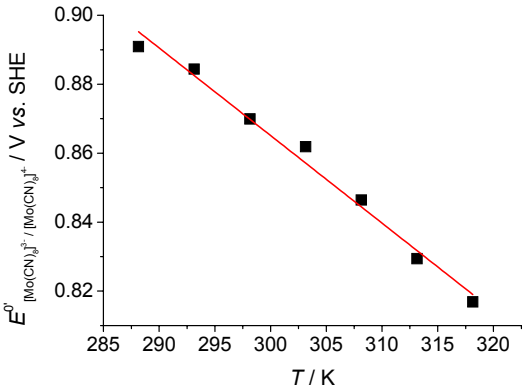


**Figure S12.** Temperature dependence of the formal potential for the reduction of 1 mM octacyanomolybdate, $I$ = 2 M ($NaClO_4$).

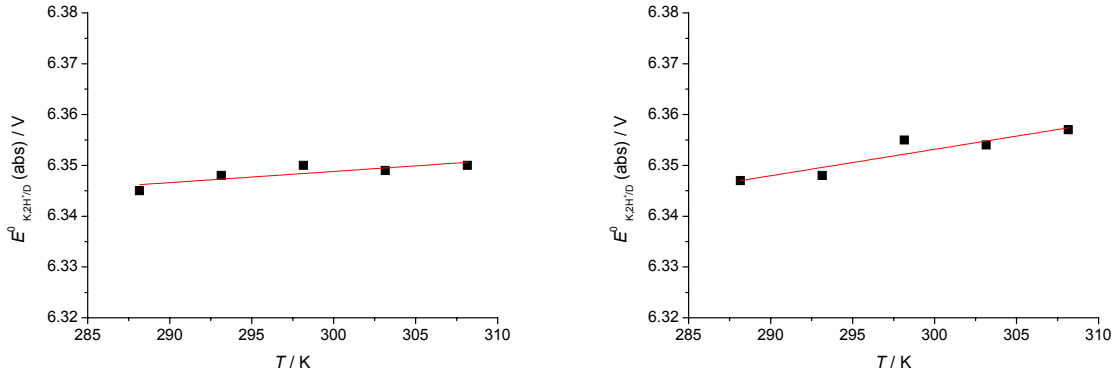


**Figure S13.** Temperature dependence of the formal potential for the redox couple K,$2H^+$/D, as assigned in Scheme 1, $I$ = 2 M ($NaClO_4$): **left:** MnTE-2-PyP, **right:** MnTE-3-PyP.

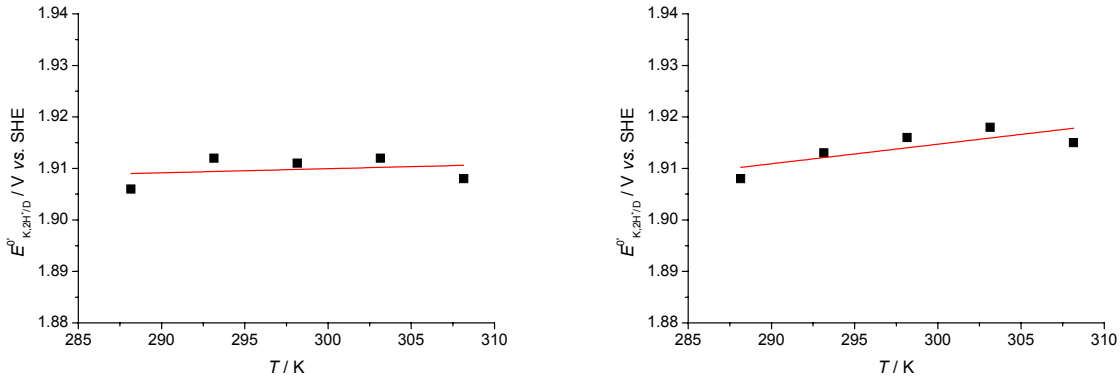


**Figure S14.** Temperature dependence of the formal potential for the redox couple K,$2H^+$/D *vs*. SHE, as assigned in Scheme 1, $I$ = 2 M ($NaClO_4$): **left:** MnTE-2-PyP, **right:** MnTE-3-PyP.

**Table S1.** Thermodynamic data for the accessible redox couples of the studied manganese porphyrin complexes obtained in 2 M $NaClO_4$. The values were calculated from absolute redox potentials.

| Couple | Parameter | |
|---|---|---|
| | $\Delta H \pm \sigma$[a] | $\Delta S \pm \sigma$[b] |
| $(O)(H_2O)Mn^{IV}$TE-2-$PyP^{4+} + 2H^+ + e^- \rightarrow (H_2O)_2Mn^{III}$TE-2-$PyP^{5+}$ | -606 ± 2 | 21 ± 7 |
| $(O)(H_2O)Mn^{IV}$TE-2-$PyP^{4+} + H^+ + e^- \rightarrow (OH)(H_2O)Mn^{III}$TE-2-$PyP^{4+}$ | -557 ± 5 | -23 ± 10 |
| $(O)(H_2O)Mn^{IV}$TE-2-$PyP^{4+} + e^- \rightarrow (O)(H_2O)Mn^{III}$TE-2-$PyP^{3+}$ | -509 ± 8 | -85 ± 21 |
| $(O)(OH)Mn^{IV}$TE-2-$PyP^{4+} + 2H^+ + e^- \rightarrow (OH)(H_2O)Mn^{III}$TE-2-$PyP^{5+}$ | -609 ± 8 | 14 ± 21 |
| $(O)(H_2O)Mn^{IV}$TE-3-$PyP^{4+} + 2H^+ + e^- \rightarrow (H_2O)_2Mn^{III}$TE-3-$PyP^{5+}$ | -598 ± 4 | 50 ± 12 |
| $(O)(H_2O)Mn^{IV}$TE-3-$PyP^{4+} + H^+ + e^- \rightarrow (OH)(H_2O)Mn^{III}$TE-3-$PyP^{4+}$ | -547 ± 7 | -1 ± 21 |
| $(O)(H_2O)Mn^{IV}$TE-3-$PyP^{4+} + e^- \rightarrow (O)(H_2O)Mn^{III}$TE-3-$PyP^{3+}$ | -496 ± 10 | -73 ± 32 |
| $(O)(OH)Mn^{IV}$TE-3-$PyP^{4+} + 2H^+ + e^- \rightarrow (OH)(H_2O)Mn^{III}$TE-3-$PyP^{5+}$ | -597 ± 13 | 58 ± 40 |

[a] Reaction enthalpies are given in kJ $mol^{-1}$. [b] Reaction entropies are given in J $K^{-1}$ $mol^{-1}$.

**Table S2.** The formal reduction potentials vs. SHE for all experimentally available redox couples assigned as in Scheme 1, obtained by the spectrophotometric pH titrations at $\theta$ = 25 °C, $I$ = 2 M ($NaClO_4$).

| $Mn^X/Mn^{X-1}$ | Redox couple | $E^{0'}$ / V | | |
|---|---|---|---|---|
| | | **MnTE-2-PyP** | **MnTE-3-PyP** | **MnTnBu-2-PyP**[a] |
| Mn(III)/Mn(II) | $D/B,H^+$ | –0.550 | –0.764 | –0.506 |
| | $E,H^+/A$ | +0.789 | +0.632 | +0.875 |
| | $F,2H^+/A$ | +1.477 | +1.384 | +1.604 |
| | $F,H^+/B$ | +0.782 | +0.671 | +0.895 |
| Mn(IV)/Mn(III) | $K,2H^+/D$ | +1.910 | +1.915 | +1.800 |
| | $K,H^+/E$ | +1.266 | +1.231 | +1.128 |
| | $L,3H^+/D$ | +2.569 | +2.624 | +2.497 |
| | $L,2H^+/E$ | +1.925 | +1.940 | +1.825 |
| | $L,H^+/F$ | +1.237 | +1.189 | +1.095 |
| Mn(IV)/Mn(II) | $K/A,2H^+$ | +1.028 | +0.932 | +1.002 |
| | $L/A,3H^+$ | +0.680 | +0.575 | +0.647 |
| | $K/B,H^+$ | +1.357 | +1.286 | +1.350 |
| | $K/B,2H^+$ | +1.009 | +0.930 | +0.995 |

[a] Values taken from Reference 13.